X-642-67-619

NASA TM X- 63087

CURRENT AND DRIVING POINT IMPEDANCE COMPUTATIONS FOR LONG RESONANT ANTENNAS

PATRICIA A. COMELLA

DECEMBER 1967

GSFC

GODDARD SPACE FLIGHT CENTER

GREENBELT, MARYLAND

X-642-67-619

CURRENT AND DRIVING POINT IMPEDANCE COMPUTATIONS FOR LONG RESONANT ANTENNAS

Patricia A. Comella

December 1967

GODDARD SPACE FLIGHT CENTER
Greenbelt, Maryland

PRECEDING PAGE BLANK NOT FILMED.

CURRENT AND DRIVING POINT IMPEDANCE COMPUTATIONS FOR LONG RESONANT ANTENNAS

Patricia A. Comella

ABSTRACT

The solution of the Hallen integral equation for a resonant cylindrical antenna is presented in a simple trigonometric form. The method of solution is discussed. A Romberg integration scheme, used in the antenna calculations, is given. The computations are discussed and a sample of results is shown.

CONTENTS

FIGURES

TABLE

CURRENT AND DRIVING POINT

IMPEDANCE COMPUTATIONS FOR

LONG RESONANT ANTENNAS

I. DESCRIPTION OF THE EQUATION

Finding a representation for the current on long cylindrical antennas that is both simple and in good agreement with more complicated formulations is difficult because such a representation is an approximate solution to the Hallen integral equation for the current, $I_z(z)$:

$$\int_{-h}^{h} I_z(z') K(z, z') \, dz' = -\frac{j\,4\pi}{\zeta_o}\left[C\cos(\beta_o z) + \tfrac{1}{2} V_o \sin(\beta_o |z|)\right] \tag{1}$$

where

$$K(z, z') = R^{-1} \exp(-j\beta_o R)$$

with

$$R = \left((z - z')^2 + a^2\right)^{\frac{1}{2}}$$

$$\zeta_o = 120 \text{ ohms}, \quad \beta_o = 2\pi/\lambda ,$$

$$a = \text{radius of the antenna}$$

$$\beta_o h = n\pi/2 \qquad n = 1, 3, \ldots .$$

$$2h = \text{length of the antenna in wavelengths}$$

The antenna is center-driven by the delta-function generator, V_o.

This is an integral equation of the first kind which has the form

$$\int_{a}^{b} f(z') K(z, z') \, dz' = h(z) ,$$

where K and h are known, f unknown, functions of z; as opposed to integral equations of the second kind which have the form

$$\int_a^b f(z')K(z,z')\,dz' + h(z) = f(z)\,,$$

where again h and K are known, f unknown.

From the viewpoint of the physicist equations of the latter type are easier to solve because a specific formulation for f does not have to be proposed before numerical methods of analysis can be meaningfully employed to obtain the desired solution. Quite the opposite with equations of the former type: experience shows that a model for f, which adequately describes the physical situation as known from experiment, must be devised before the parametric values obtained in the approximate solution will yield a good fit to the experimental data. That is, no amount of mathematical analysis, however excellent can make a poor model for f yield good results.

Using experimental data as a guide, King and Sandler(3) have derived a simple trigonometric current representation for long resonant antennas. The antenna current consists of a shifted sine and cosine distribution with coefficients A and B. It has the following final form:

$$I_z(z) = -jA\cos\left[\beta_o(z-m_o)\right] + B\cos(\beta_o z) + g(z,m_o) \tag{2}$$

where

$$A = 2\pi/\left[\zeta_o\varphi_{CR}(m_o)\sin(\beta_o m_o)\right] \tag{3}$$

$$B = jA\left[\varphi_{C1}(h) + \varphi_C' - \varphi_{CR}(m_o)\cos\left\{\beta_o(h-m_o)\right\}\right]/\varphi_{C2}(h) \tag{4}$$

$$g(z,m_o) = -jA\Big[\cos\left\{\beta_o(h-2m_o)\right\}\cos(\beta_o z)/\cos\left\{\beta_o(h-m_o)\right\} - \cos\left\{\beta_o(z-m_o)\right\}\Big] \quad h-m_o \le z \le h \tag{5}$$

$$g(z,m_o) = 0 \qquad 0 \le z < h-m_o$$

$$\varphi_{CR}(m_o) = \text{REAL}\left[\cos(\beta_o m_o) C_a(h, m_o) - \sin(\beta_o m_o) S_a(h, m_o)\right] \tag{6}$$

$$\varphi_{C1}(h) = \cos(\beta_o m_o) C_a(h-m_o, h) + \sin(\beta_o m_o) S_a(h-m_o, h) \tag{7}$$

$$\varphi_{C2}(h) = C_a(h, h) \tag{8}$$

$$\varphi'_C = C_a(h, h) - C_a(h-m_o, h) \tag{9}$$

$$C_a(h, z) = \int_{-h}^{h} \cos(\beta_o z') K(z, z') dz' \tag{10}$$

$$S_a(h, z) = \int_{-h}^{h} \sin(\beta_o |z'| K(z, z') dz' \tag{11}$$

The phase shift m_o must be determined from a transcendental equation given by

$$\text{Cos}(\beta_o m_o) - \sin(\beta_o m_o) = - \text{REAL}\left[\varphi_{C2}^{-1}(h)\left\{\varphi_{C1}(h) + \varphi'_C - \varphi_{CR}(m_o)\cos\beta_o(h-m_o)\right\}\right]. \tag{12}$$

Once the value of m_o is calculated, A and B can then be determined from Equations (3) and (4).

The first model for the current gave a poor fit to the experimental data because (5) was not well formulated. Consequently, this equation was modified so that the final representation for $I_z(z)$ compared excellently with both experimentally obtained and theoretically calculated currents.[3]

II. METHOD OF SOLUTION

The function $f(m)$ is defined by

$$f(m) = \cos(\beta_o m) - \sin(\beta_o m) + \text{REAL}\left[\varphi_{C2}^{-1}(h) \left\{ \varphi_{C1}(h) + \varphi_C' - \varphi_{CR}(m) \cos\left\{ \beta_o (h-m) \right\} \right\} \right]. \tag{13}$$

Clearly, a zero of (13) is a solution of (12). From physical considerations m_o is such that $0 < m_o < .25$.

The Newton-Raphson method with suitable restrictions to insure that m_i was in the first quadrant for $i = 1, 2, \ldots, N$, was chosen to find m_o. This is an iterative procedure of the form

$$m_{i+1} = m_i - f(m_i)/f'(m_i), \quad i = 1, 2, \ldots, N. \tag{14}$$

The recursion formula is given by setting $\phi(m) = m - f(m)/f'(m)$. The resulting relation $m_{i+1} = \phi(m_i)$ is the recursion formula. The sequence $\{m_n\}$ converges to the fixed point, $m_o = \phi(m_o)$, of ϕ provided that m_1 is sufficiently close to m_o, that $\phi'(m)$ is continuous in an interval around m_o, and that $|\phi'(m_o)| < 1.$[5] In the Newton-Raphson method $\phi'(m) = f(m) f''(m)/(f'(m))^2$, so that $\phi'(m_o) = 0$ provided that f is twice continuously differentiable and that $f'(m_o) \neq 0$.

The analytic expression for $f'(m)$ would be extremely difficult (and tedious) to find and equally cumbersome to programe for evaluation. Thus the derivative of $f(m)$ was approximated by the difference formula

$$f'(m) = \frac{f(m + \Delta m) - f(m)}{\Delta m}, \tag{15}$$

where Δm was sufficiently small.

All integrals were evaluated numerically. A set of recursion formulas, called a Romberg scheme for Simpson sums, was used. The method is based on repeated interval halving until the desired degree of accuracy is reached.

III. ROMBERG SCHEME FOR NUMERICAL INTEGRATION[5]

This section outlines a quadrature scheme, based on interval halving, which evaluates numerically the definite integral $\int_a^b f(x)\,dx$, where f (x) is a continuous function that can be calculated by some means at any point x. (To facilitate discussion the interval [a,b] is normalized to [0,1] by a suitable transformation on x). First a recursion formula for trapezoidal sums is described. The trapezoidal rule for mesh size, h, gives the approximation, T, to $\int_0^1 f(x)\,dx$:

$$T = \frac{h}{2}\left[f(o) + 2\left\{f(h) + f(2h) + \ldots + f(1-h)\right\} + f(1)\right].^{(4)}$$

The recursion expresses the i^{th} trapezoidal sum, T_i, of mesh-size, $h = (\frac{1}{2})^{i-1}$, as $\frac{1}{2}$ the sum of T_{i-1} and the mean of the values f (x) when x takes on the values $(2j - 1)/2^{i-1}$, $j = 1, 2, \ldots, 2^{i-2}$. Then a second recursion formula is derived to express the i^{th} Simpson sum, S_i, of mesh-size, $h = (\frac{1}{2})^{i}$, as a linear combination of T_{i+1} and T_i. Simpson's rule approximates $\int_0^1 f(x)\,dx$ by the sum, S,

$$S = \frac{h}{3}\left[f(o) + 4\left\{f(h) + f(3h) + \ldots + f(1-h)\right\}\right.$$

$$\left. + 2\left\{f(2h) + \ldots + f(1-2h)\right\} + f(1)\right],^{(4)}$$

for the mesh, h.

This recursive method has the outstanding advantage that as one decreases the mesh size from $(\frac{1}{2})^n$ to $(\frac{1}{2})^{n+1}$, one need compute only 2^n new points, instead of the $2^{n+1} + 1$ points usually computed. Thus, computation time is saved. Furthermore, the mesh-size can be made a function of the convergence criterion.

In Figure 1, the area of trapezoid ACDF, denoted by $T(\frac{1}{2})$, $\frac{1}{2}$ being the midpoint of its base along the X-axis, is a rough approximation to the area under the curve $y = f(x)$ in the interval [0,1]. Define

$$T_1 = T(\tfrac{1}{2}) = \tfrac{1}{2}\left[f(o) + f(1)\right] \tag{16}$$

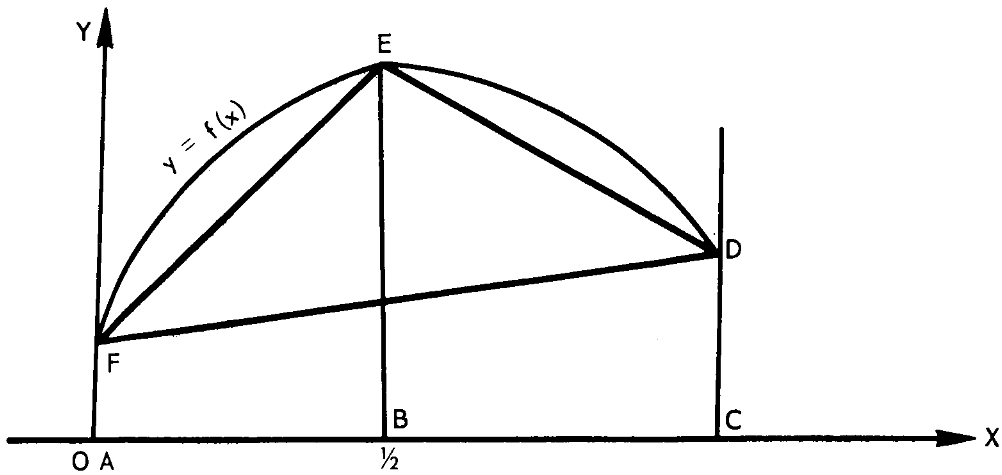

Figure 1.

Hopefully the sum of the area of trapezoid ABEF, denoted by $T(\frac{1}{4})$; and of BCDE, designated $T(\frac{3}{4})$, is a better approximation, T_2, to the desired area. Thus, if $T(\frac{1}{4})$, $T(\frac{3}{4})$ and T_2 are defined by the following relations

$$T(\tfrac{1}{4}) = \tfrac{1}{4}\left[f(o) + f(\tfrac{1}{2})\right]$$

$$T(\tfrac{3}{4}) = \tfrac{1}{4}\left[f(\tfrac{1}{2}) + f(1)\right] \tag{17}$$

$$T_2 = T(\tfrac{1}{4}) + T(\tfrac{3}{4}) = \tfrac{1}{2}\left[T_1 + f(\tfrac{1}{2})\right]$$

it is hoped that

$$\left|\int_0^1 f(x)\,dx - T_2\right| \leqq \left|\int_0^1 f(x)\,dx - T_1\right|$$

In the same manner the area under $y = f(x)$ may be approximated by the four trapezoidal areas:

$$T(\tfrac{1}{8}) = \tfrac{1}{8}\left[f(0) + f(\tfrac{1}{4})\right]$$

$$T(\tfrac{3}{8}) = \tfrac{1}{8}\left[f(\tfrac{1}{4}) + f(\tfrac{1}{2})\right]$$

$$T(\tfrac{5}{8}) = \tfrac{1}{8}\left[f(\tfrac{1}{2}) + f(\tfrac{3}{4})\right] \qquad (18)$$

$$T(\tfrac{7}{8}) = \tfrac{1}{8}\left[f(\tfrac{3}{4}) + f(1)\right]$$

The sum of these areas in (18) is T_3 where

$$T_3 = \tfrac{1}{2}\left[T_2 + \frac{f(\tfrac{1}{4}) + f(\tfrac{3}{4})}{2}\right] \qquad (19)$$

Using the first inductive principle one can prove that if

$$T_1 = \tfrac{1}{2}\left[f(0) + f(1)\right]$$

then

$$T_i = \tfrac{1}{2}\left[T_{i-1} + \sum_{j=1}^{N} f\left(\frac{2*j-1}{M}\right)/N\right], \quad i = 2,\ 3,\ \ldots. \qquad (20)$$

where

$$N = 2^{i-2}, \quad M = 2^{i-1}$$

For the unnormalized interval [a,b]

$$T_1 = \frac{b-a}{2}\left[f(a) + f(b)\right]$$

and

$$T_i = \frac{b-a}{2}\left[\frac{T_{i-1}}{b-a} + \sum_{j=1}^{N} f\left(a + \left\{\frac{2*j-1}{M}\right\}\{b-a\}\right)/N\right] \quad i = 2, 3, \ldots. \qquad (20')$$

where

$$N = 2^{i-2}, \; M = 2^{i-1}$$

It is obvious that

$$\lim_{n\to\infty} T_n = \int_a^b f(x)\,dx \tag{21}$$

The following paragraphs will now establish a linear relationship between elements of the sequence $\left\{\frac{S}{n}\right\}$ of successive approximations to the definite integral $\int_0^1 f(x)\,dx$ using Simpson's rule and the elements of the sequence $\{T_i\}$ of successive approximations using the trapezoidal rule.

In mechanical quadrature $f(x)$ is replaced by an interpolating formula integrated between the limits, a and b, (in this discussion 0 and 1), of the definite integral. For Simpson's rule the interpolating formula is a polynomial of degree 2, denoted $P_2(x)$. Therefore, a linear combination, S_1, of T_1 and T_2, is required which yields exactly the value of the definite integrals, $\int_0^1 P_2(x)\,dx$.

For example, if $f(x) = x^2$,

$$\int_0^1 x^2\,dx = \tfrac{1}{3} = pT_1 + qT_2 \tag{22}$$

with $p + q = 1$. Since $T_1 = \frac{1}{2}$, $T_2 = \frac{3}{8}$, the following system of linear equations is solved:

$$p + q = 1$$

$$p/2 + \tfrac{3}{8}q = \tfrac{1}{3} \tag{23}$$

obtaining $p = -\frac{1}{3}$, $q = \frac{4}{3}$, so that

$$S_1 = (4T_2 - T_1)/3 \tag{24}$$

Geometrically, Simpson's rule replaces f(x) by parabolas (the trapezoidal rule, by chords), as follows: for a mesh of $\frac{1}{2}$, a parabola, denoted by $P_{2,\frac{1}{2}}(x)$*, is passed through the points $(0, f(0))$, $(\frac{1}{2}, f(\frac{1}{2}))$, $(1, f(1))$, which replaces f(x) in the interval [0,1]. Thus, $\int_0^1 f(x)\,dx$ is approximated by $\int_0^1 P_{2,\frac{1}{2}}(x)\,dx$. If the interval [0,1] is divided into quarters, f(x) can be approximated by the sum of two parabolas, $P_{2,\frac{1}{4}}(x)$ through the points $(0, f(0))$, $(\frac{1}{4}, f(\frac{1}{4}))$, $(\frac{1}{2}, f(\frac{1}{2}))$; and $P_{2,\frac{3}{4}}(x)$ through $(\frac{1}{2}, f(\frac{1}{2}))$, $(\frac{3}{4}, f(\frac{3}{4}))$, $(1, f(1))$. Integrating this sum one obtains, using (24) and (20') for intervals of length $\frac{1}{2}$, the approximation, S_2, to $\int_0^1 f(x)\,dx$,

$$S_2 = (4T_3 - T_2)/3 \tag{25}$$

since

$$T_1' = \frac{1}{4}\left[f(o) + f(\tfrac{1}{2})\right] \qquad T_1'' = \frac{1}{4}\left[f(\tfrac{1}{2}) + f(1)\right]$$

$$T_2' = \frac{1}{4}\left[2T_1' + f(\tfrac{1}{4})\right] \qquad T_2'' = \frac{1}{4}\left[2T_1'' + f(\tfrac{3}{4})\right]$$

$$S_1' = (4T_2' - T_1')/3 \qquad S_2'' = (4T_2'' - T_1'')/3$$

$$S_2 = S_1' + S_1'' = \left[T_1' + T_1'' + f(\tfrac{1}{4}) + f(\tfrac{3}{4})\right]/3 = (4T_3 - T_2)/3$$

where

' applies to sums on the interval $[0,\frac{1}{2}]$,

" to sums on $[\frac{1}{2},1]$.

By dividing the interval [0,1] into eighths, it can be shown that

$$S_3 = (4T_4 - T_3)/3.$$

*$P_{2,m}(x)$ is a parabola which replaces f(x) in the sub-interval with midpoint, m.

Generally, the recursion relation is of the form

$$S_i = (4T_{i+1} - T_i)/3. \tag{26}$$

The sequence $\{S_n\}$ is a sequence of successive approximations to $\int_o^1 f(x)\,dx$, using Simpson's rule with mesh-size $h = h_n = 2^{-n}$.

To utilize the Romberg method in evaluating integrals of the form $\int_a^b f(x)\,dx$, a S/360 Fortran IV program was written. It is available from the Goddard Program Library. (2) This program is especially recommended in cases where an optimal, but unknown, mesh-size is needed in order to approximate an integral to a pre-determined number of significant figures. Test cases indicate that up to six figures of accuracy can be obtained using this program.

IV. DISCUSSION OF COMPUTATIONS AND RESULTS

The computations were done on the IBM 7094-7040 DCS and the IBM S/360 ASP systems at Goddard Space Flight Center. The IBM S/360 Fortran IV, Version H, program of the King-Sandler theory is documented and available from the Goddard Program Library. (1)

To evaluate the functions containing integrals, (10) and (11) were split into their real and imaginary parts. Each of the resulting integrals was then approximated separately using Program No. M00077 in the Goddard Program Library. This program utilizes the method discussed in Section III.

Successive approximations, S_i and S_{i+1}, to an integral, I, were tested for convergence as follows:

given ϵ, if

$$|(S_i - S_{i+1})/S_i| < \epsilon, \tag{27}$$

then

$$I = S_{i+1}$$

For all of the results given in this paper $\epsilon = 10^{-3}$ was chosen because:

1) if $\epsilon > 10^{-3}$, the m_o obtained in the solution of (13) differed significantly from the m_o for $\epsilon = 10^{-3}$;

2) the m_o obtained for $\epsilon < 10^{-3}$ agreed to three figures with that for $\epsilon = 10^{-3}$, but the computational times differed greatly.

In the Newton-Raphson iterative procedure zero was approximated by 10^{-3}; that is, if $f(m_i) < 10^{-3}$, $m_o = m_i$ the desired zero of (13). Once again this criterion was established empirically: such a tolerance seemed to give an optimal trade-off between time and accuracy. Similar considerations indicated that $\Delta m = 10^{-3}$ be used in (15).

Each iteration required two evaluations of (13) which, in turn, was a function of the integrals given by (6), (7), (8), (9). On the IBM S/360 ASP, 57.5 seconds were required to evaluate (13). An average of 5.3 iterations was needed for the convergence of the sequence $\{m_i\}$ to m_o.

However, a good estimate for m_1/λ shortened the number of iterations to one or two; while a bad estimate caused an end of case condition to occur. To facilitate the selection of m_1/λ for a given h/λ, a plot of m_o/λ as a function of h/λ was made for completed cases. Figure 2 shows such a graph for $\Omega = 20$. Since Line I appeared to be an upper bound for the points $(h/\lambda, m_o/\lambda)$; and Line II a lower bound, $(h/\lambda, m_1/\lambda)$ less than (or equal to) the corresponding point on Line I and greater than (or equal to) that on Line II was chosen as the starting point.

Table I summarizes the King-Sandler results for $\Omega = 20$. For a given half-length, h/λ, the phase shift, m_o/λ, the driving point admittance, Y_o, the driving-point impedance, Z_o, and the coefficients, A and B, calculated using (3) and (4), respectively, are tabulated. All computations are to four significant figures. The parametric values of h/λ, m_o/λ, A and B can then be used in (2) to compute the current at any point along the antenna.

The good agreement between the King-Sandler approximate model and the experiments of Altshuler and theories of Wu and King-Middleton for selected values of h and Ω indicates that this model is an adequate description of currents on long resonant antennas.

ACKNOWLEDGMENTS

I wish to thank Dr. Sheldon S. Sandler for the opportunity to work on this problem; Dr. Arnold P. Stokes and Mr. William F. Cahill for their encouragement and suggestions.

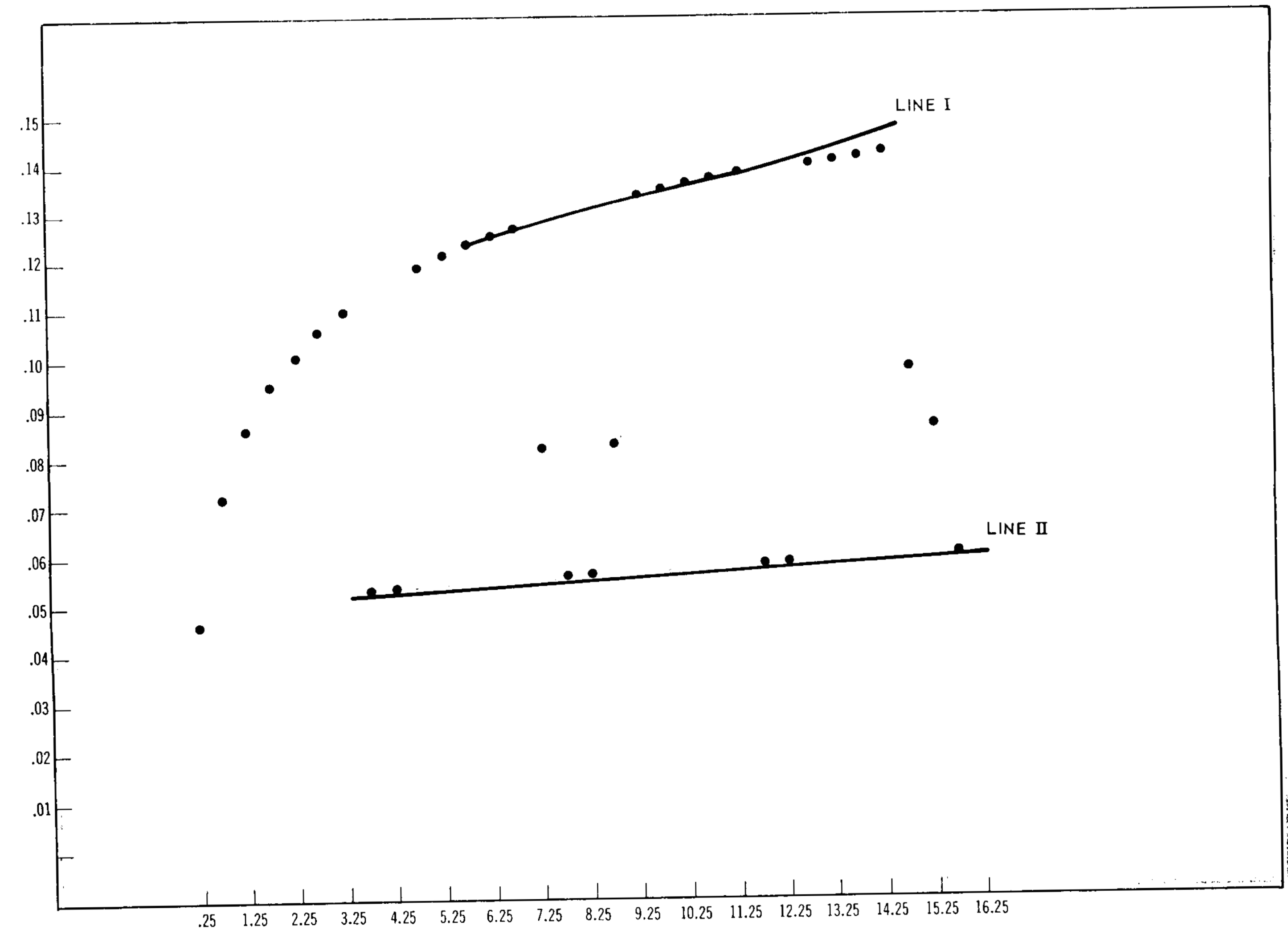

Figure 2. Phase Shift as a Function of Antenna Half-length for $\Omega = 20$.
Units of Wavelength

Table I

Resonant Antenna Parameters

A, B, Y_o in milliohms, Z_o in ohms

$\Omega = 20$

h/λ	m_o/λ	Y_o	Z_o	A	B
0.25	0.0455	10.08 - j5.23	78.2 + j40.6	3.19	10.08 - j5.23
0.75	0.0719	7.70 - j3.04	112.3 + j44.4	2.23	7.70 - j1.03
1.25	0.0853	6.86 - j2.42	129.7 + j45.8	2.00	6.86 - j0.70
1.75	0.0941	6.37 - j2.09	141.7 + j46.6	1.90	6.37 - j0.52
2.25	0.1005	6.03 - j1.88	151.1 + j47.2	1.84	6.03 - j0.40
2.75	0.1056	5.78 - j1.73	158.9 + j47.6	1.80	5.78 - j0.31
3.25	0.1098	5.57 - j1.62	165.6 + j48.0	1.78	5.57 - j0.24
3.75	0.0521	8.68 - j5.29	84.0 + j51.2	3.36	8.68 - j2.11
4.25	0.0526	8.62 - j5.27	84.4 + j51.6	3.36	8.62 - j2.09
4.75	0.1189	5.14 - j1.38	181.5 + j48.1	1.76	5.14 - j0.10
5.25	0.1212	5.03 - j1.33	185.9 + j49.1	1.75	5.03 - j0.06
5.75	0.1233	4.93 - j1.28	190.0 + j49.4	1.75	4.93 - j0.03
6.25	0.1251	4.84 - j1.24	193.9 + j49.6	1.75	4.84 + j0.00
6.75	0.1267	4.76 - j1.20	197.5 + j49.7	1.76	4.76 + j0.03
7.25	0.0813	6.90 - j3.02	121.6 + j53.2	2.40	6.90 - j0.92
7.75	0.0553	8.36 - j5.18	86.5 + j53.6	3.36	8.36 - j2.02
8.25	0.0555	8.33 - j5.17	86.7 + j53.8	3.36	8.33 - j2.01
8.75	0.0823	6.83 - j3.01	122.7 + j54.1	2.42	6.83 - j0.91
9.25	0.1333	4.45 - j1.05	213.0 + j50.5	1.77	4.45 + j0.13
9.75	0.1344	4.39 - j1.03	215.7 + j50.6	1.78	4.39 + j0.15
10.25	0.1354	4.35 - j1.01	218.3 + j50.7	1.78	4.35 + j0.17
10.75	0.1364	4.30 - j0.99	220.9 + j50.8	1.79	4.30 + j0.18
11.25	0.1373	4.26 - j0.97	223.3 + j50.9	1.79	4.26 + j0.19
11.75	0.0573	8.17 - j5.10	88.1 + j55.2	3.36	8.17 - j1.96
12.25	0.0576	8.15 - j5.09	88.2 + j55.2	3.36	8.15 - j1.95
12.75	0.1396	4.14 - j0.92	230.2 + j51.2	1.81	4.14 - j0.23
13.25	0.1403	4.10 - j0.91	232.4 + j51.3	1.81	4.10 - j0.25
13.75	0.1410	4.07 - j0.89	234.5 + j51.4	1.82	4.07 - j0.26
14.25	0.1417	4.03 - j0.88	236.6 + j51.5	1.82	4.03 - j0.27
14.75	0.0976	6.00 - j2.38	144.1 + j57.2	2.25	6.00 - j0.54
15.25	0.0857	6.59 - j2.97	126.2 + j56.9	2.47	6.59 - j0.85
15.75	0.0592	7.69 - j5.01	89.9 + j56.5	3.34	7.97 - j1.90

REFERENCES

1. P. A. Comella, "Currents, Driving-Point Impedances and Admittances on Long Resonant Antennas," Goddard Space Flight Center Computer Program Library, Program No. M00078.

2. P. A. Comella, "Romberg Integration Scheme," Goddard Space Flight Center Computer Program Library, Program No. M00077.

3. R. W. P. King and S. S. Sandler, "Driving-Point Impedance and Current for Long Resonant Antennas, IEEE Trans. on Antennas and Propagation," Vol. AP-14, pp. 639-641, September, 1966.

4. J. B. Scarborough, "Numerical Mathematical Analysis." Baltimore: The John Hopkins Press, 1962.

5. E. L. Stiefel, "An Introduction to Numerical Mathematics." New York: Academic Press, 1963, Ch. 4.2, 4.3, Ch. 6.2.